Available online at www.sciencedirect.com

ScienceDirect

Coastal Engineering 54 (2007) 856–864

Coastal Engineering
An International Journal for Coastal, Harbour and Offshore Engineers

www.elsevier.com/locate/coastaleng

Bottom friction and its effects on periodic long wave propagation

A. Orfila [a,*], G. Simarro [b], P.L.F. Liu [c]

[a] IMEDEA(CSIC-UIB), Miquel Marques, 21, 07190 Esporles, Spain
[b] ETS Caminos Canales y Puertos, UCLM, 13071 Ciudad Real, Spain
[c] School of Civil and Env. Eng. Cornell University, 14853 Ithaca, NY, United States

Received 14 November 2005; received in revised form 23 April 2007; accepted 24 May 2007
Available online 12 July 2007

Abstract

A new set of Boussinesq-type equations describing the free surface evolution and the corresponding depth-integrated horizontal velocity is derived with the bottom boundary layer effects included. Inside the boundary layer the eddy viscosity gradient model is employed to characterize Reynolds stresses and the eddy viscosity is further approximated as a linear function of the distance measured from the seafloor. Boundary-layer velocities are coupled with the irrotational velocity in the core region through boundary conditions. The leading order boundary layer effects on wave propagation appear in the depth-integrated continuity equation to account for the velocity deficit inside the boundary layer. This formulation is different from the conventional approach in which a bottom stress term is inserted in the momentum equation. An iterative scheme is developed to solve the new model equations for the free surface elevation, depth-integrated velocity, the bottom stress, the boundary layer thickness and the magnitude of the turbulent eddy viscosity. A numerical example for the evolution of periodic waves propagating in one-dimensional channel is discussed to illustrate the numerical procedure and physics involved. The differences between the conventional approach and the present formulation are discussed in terms of the bottom frictional stress and the free surface profiles.

Keywords: Turbulent boundary layer; Boussinesq approximation; Bottom friction; Eddy viscosity

1. Introduction

For long water waves traveling over a long distance bottom frictional effects become important. The turbulence generated inside the bottom boundary layer will not only attenuate wave energy, but also modify wave form and wave speed. To include the effects of bottom friction in wave models, a bed shear term is traditionally added to the depth-integrated momentum equations and the bottom shear stress is then modeled as a function of the velocity above the bed. Most of existing models further assume that the shear stress is in phase with the near bed velocity. However, it is well known that for a laminar boundary layer, the phase lag between the bottom shear stress and the bed velocity is $\pi/4$ (Mei, 1989). Recently, Liu and Orfila (2004) (this paper will be referred as LO hereafter) derived a set of depth-integrated continuity and momentum equations with boundary-layer effects considered for long-wave propagation. Considering the viscosity as a constant, LO showed that the leading-order boundary-layer effect appears in the depth-integrated continuity equation as a correction term representing the velocity deficit in the boundary layer (Lighthill, 1978). The correction term is expressed as a convolution integral and therefore, bottom frictional effects have a memory in time. Liu et al. (2006) solved LO's Boussinesq-type equations to examine the damping and shoaling of solitary waves. Laboratory experiments in a wave flume were conducted and experimental data confirmed that LO's formulation is accurate. More recently, using the PIV technique, Liu et al. (2007) measured the boundary layer velocity and bottom shear stress under solitary waves and showed that experimental data agreed with LO's formulae very well. We remark here that in the laboratory experiments the boundary layers are indeed laminar. However, the theoretical formulation developed by LO can be applied to a turbulent boundary layer with the limitation of a constant eddy viscosity. More recently, Torsvik and Liu (2007) presented an

* Corresponding author. Tel.: +34 971611834.
E-mail address: a.orfila@uib.es (A. Orfila).

0378-3839/$ - see front matter © 2007 Elsevier B.V. All rights reserved.
doi:10.1016/j.coastaleng.2007.05.013

efficient and accurate procedure to evaluate the convolution integral.

For a fully developed turbulent boundary layer, many researchers have suggested that the eddy viscosity model is adequate and the eddy viscosity can be modeled as a power function of the distance measured from the bottom. Adopting this eddy viscosity model, Liu (2006) derived another set of Boussinesq-type wave equations with the turbulent boundary layer effects included. However, in Liu's (2006) derivation a coordinate transformation was used such that the theory becomes invalid when the eddy viscosity becomes a linear function of the distance from the bottom (Kajiura, 1968; Jonsson and Carlsen, 1976; Grant and Madsen, 1979), i.e.

$$\nu'_t(\zeta') = \kappa|\mathbf{u}'_*|\zeta', \tag{1}$$

where ζ' is the local coordinate normal to the sea bottom, κ the von Karman constant ($\sim$0.40), and $\mathbf{u}'_*$ the frictional velocity, which is related to the bottom stress. In this paper we shall extend LO's model to include the effects of a fully developed turbulent bottom boundary layer, in which the eddy viscosity model given in (1) can be used. Furthermore, we shall focus only on periodic waves without leading order currents.

The paper is structured in the following manner. For completeness we first summarize the governing equations and boundary conditions for the long wave propagation in Section 2. The Boussinesq-type equations are derived in Section 3. These equations are expressed in terms of the Fourier (harmonic) components of the free surface displacement and the depth-averaged horizontal velocity. The effects of the boundary layer are described. Section 4 presents the analysis for turbulent boundary layer under an oscillatory flow. In particular, the expressions for boundary layer thickness and bottom stress are given. We need to point out that the boundary layer thickness is a part of the solution. Once the relationship between the boundary-layer solution and the depth-averaged velocity is found, the Boussinesq-type equations presented in Section 3 can be combined into one set of equations in terms of the free surface displacement. The final equations are presented in Section 5. Numerical results for a sinusoidal wave propagating in a numerical tank are shown in Section 6. The effects of turbulent boundary layer on the evolution of different harmonics are discussed. Finally, Section 7 concludes the paper.

2. Governing equations and boundary conditions

In this paper, we consider a periodic wave train with the surface displacement $\eta'(x', y', t')$ propagating in a constant water depth, h'_0. The wave train is characterized by a typical wave amplitude, a'_0, its fundamental frequency, ω'_0, and the corresponding wave number, $k'_0 = \omega'_0/\sqrt{g'h'_0}$. The following dimensionless variables are introduced:

$$\begin{aligned}(x,y) &= k'_0(x',y'), \quad z = z'/h'_0, \quad t = \omega'_0 t'\\ \eta &= \eta'/a'_0, \quad p = p'/\rho' g' a'_0,\\ (u,v) &= (u',v')/\epsilon\sqrt{g'h'_0}, \quad w = \mu w'/\epsilon\sqrt{g'h'_0},\end{aligned} \tag{2}$$

in which p' denotes the pressure, (u', v') the horizontal velocity components in the (x', y') directions, w' the velocity component in the z' direction, ρ' the fluid density, and g' the gravitational acceleration. Two dimensionless parameters have been introduced in the dimensionless variables:

$$\epsilon = a'_0/h'_0, \mu = k'_0 h'_0. \tag{3}$$

As explained in LO, the dynamics of the interactions between surface waves and boundary layer flows can be described as follows. The flow motions are essentially irrotational except in the boundary layer adjacent to the seafloor, $z' = -h'$. In order to satisfy the no-slip boundary condition on the bottom, the leading order of magnitude of the horizontal rotational velocity components inside the bottom boundary layer must be the same as that of the irrotational velocity, i.e., $O(1)$. From the continuity equation, a vertical rotational velocity component is generated inside the bottom boundary layer, which is no longer zero at the bottom. Therefore, to satisfy the no flux boundary condition on the bottom, the irrotational flow in the core region must be modified, feeling the effects of bottom boundary layer.

In the core region where the flow is assumed to be irrotational, a velocity potential Φ is introduced. The continuity equation in dimensionless form becomes,

$$\mu^2\nabla^2\Phi + \frac{\partial^2\Phi}{\partial z^2} = 0, \quad -1<z<\epsilon\eta, \tag{4}$$

and the free surface kinematic and dynamic boundary conditions are,

$$\frac{\partial\eta}{\partial t} + \epsilon\nabla\eta\cdot\nabla\Phi = \frac{1}{\mu^2}\frac{\partial\Phi}{\partial z}, \quad z = \epsilon\eta. \tag{5}$$

$$\frac{\partial\Phi}{\partial t} + \frac{\epsilon}{2}\left\{|\nabla\Phi|^2 + \frac{1}{\mu^2}\left(\frac{\partial\Phi}{\partial z}\right)^2\right\} + \eta = 0, \ z = \epsilon\eta. \tag{6}$$

At the sea bottom the no-slip and no-flux boundary conditions are required. Defining the horizontal and vertical components of the rotational velocity inside the bottom boundary layer as $\mathbf{u}_r$ and u_ζ, respectively, the boundary conditions can be expressed as

$$\nabla\Phi = -\mathbf{u}_r, \quad z = -1. \tag{7}$$

$$\frac{\partial\Phi}{\partial z} = -u_\zeta, \quad z = -1. \tag{8}$$

These boundary conditions serve as the link between core region flows and boundary layer flows. The boundary layer flows are driven by the no-slip condition, while the feedback from the boundary layer to the core-region is through the no-flux condition.

3. Boussinesq-type equations

In this section, we shall present simplified governing equations for the irrotational flows by adopting the Boussinesq approximation, i.e., $O(\epsilon) \sim O(\mu^2)$.

The primary difference between the traditional Boussinesq equations and the present problem is that the vertical component of the irrotational velocity at the bottom is not zero in the present situation. Following LO's approach, we expand the potential function as a power series in the vertical coordinate,

$$\Phi(\mathbf{x}, z, t) = \sum_{n=o}^{\infty} (z+1)^n \phi_n(x, t). \tag{9}$$

Substituting the expansion into the Laplace Eq. (4), and the bottom boundary conditions, (7) and (8), we obtain the following recursive relation:

$$\phi_{n+2} = \frac{-\mu^2 \nabla^2 \phi_n}{(n+1)(n+2)}, \tag{10}$$

with

$$\phi_1 = -u_\varsigma. \tag{11}$$

where the boundary layer effects are introduced through the velocity potential ϕ_1. Thus, using the recursive relation in the expansion, we get the potential function truncated up to $O(\mu^5)$

$$\Phi = \phi_0 + (z+1)\phi_1 - \frac{\mu^2}{2}(z+1)^2 \nabla^2 \phi_0 + \frac{\mu^4}{24}(z+1)^4 \nabla^2 \nabla^2 \phi_0 + O(\mu^6). \tag{12}$$

We reiterate here that the rotational velocity, u_ζ, which appears in ϕ_1 in (11), is expected to be greater than $O(\mu^5)$ and is to be determined from the boundary-layer analysis in Section 4. Defining the depth-averaged velocity as,

$$\bar{\mathbf{u}} = \frac{1}{1+\epsilon\eta} \int_{-1}^{\epsilon\eta} \nabla \Phi \, dz, \tag{13}$$

the depth-integrated momentum and continuity equations can be derived following LO, from the free surface boundary conditions, (5) and (6),

$$\frac{\partial \bar{\mathbf{u}}}{\partial t} + \frac{\epsilon}{2} \nabla(\bar{\mathbf{u}} \cdot \bar{\mathbf{u}}) + \nabla \eta - \frac{\mu^2}{3} \nabla \left(\nabla \cdot \frac{\partial \bar{\mathbf{u}}}{\partial t} \right) = O(\mu^4), \tag{14}$$

$$\nabla \cdot \{(1+\epsilon\eta)\bar{\mathbf{u}}\} + \frac{\partial \eta}{\partial t} + \frac{u_\varsigma}{\mu^2} = O(\mu^4). \tag{15}$$

In this paper we shall focus only on periodic waves with a fundamental frequency ω_0'. The free surface displacement and the velocity field can be expressed as a Fourier series in time,

$$\eta = \frac{1}{2} \sum_n \eta_n \exp(\mathrm{int}), \quad n = 0, \pm 1, \pm 2, \ldots \tag{16}$$

$$\bar{\mathbf{u}} = \frac{1}{2} \sum_n \bar{\mathbf{u}}_n \exp(int), \quad n = 0, \pm 1, \pm 2, \ldots \tag{17}$$

$$u_\varsigma = \frac{1}{2} \sum_n u_{\varsigma, n} \exp(\mathrm{int}), \quad n = 0, \pm 1, \pm 2, \ldots \tag{18}$$

where (η_{-n}, $\bar{\mathbf{u}}_{-n}$, $u_{\zeta,-n}$) are the complex conjugates of (η_{-n}, $\bar{\mathbf{u}}_{-n}$, $u_{\zeta,n}$). $\mathbf{u}_0$ and η_0 represent the mean velocity and the mean free surface elevation, respectively. In the present study, we assume that the mean flow field is generated only through the nonlinearity.

Introducing (16), (17) and (18) into (14) and (15) and collecting the different Fourier components, we have

$$in\bar{\mathbf{u}}_n + \frac{\epsilon}{4} \sum_s \nabla(\bar{\mathbf{u}}_s \cdot \bar{\mathbf{u}}_{n-s}) + \nabla \eta_n - \frac{in\mu^2}{3} \nabla(\nabla \cdot \bar{\mathbf{u}}_n) = O(\mu^4), \tag{19}$$

$$in\eta_n + \frac{\epsilon}{2} \sum_s \nabla \cdot (\eta_s \bar{\mathbf{u}}_{n-s}) + \nabla \cdot \bar{\mathbf{u}}_n + \frac{u_{\varsigma,n}}{\mu^2} = O(\mu^4), \tag{20}$$

for $n \neq 0$. The leading order of magnitude of mean velocity and mean free surface elevation is $O(\epsilon)$. If the mean free surface setdown in deep water is zero, the mean velocity and mean surface elevation can be calculated as (Mei, 1989):

$$\eta_0 = -\frac{\epsilon}{4} \sum_{s \neq 0} (\bar{\mathbf{u}}_s \cdot \bar{\mathbf{u}}_{-s}) + O(\mu^4). \tag{21}$$

$$\bar{\mathbf{u}}_0 = -\frac{\epsilon}{2} \sum_{s \neq 0} (\eta_s \bar{\mathbf{u}}_{-s}) + O(\mu^3). \tag{22}$$

Thus, (19) and (20) constitute the governing equations for $\bar{\mathbf{u}}_n$ and η_n ($n \neq 0$) and (21) and (22) are used to calculate the mean flow field.

For future use, we also note that for $n \neq 0$

$$\bar{\mathbf{u}}_n = \frac{i}{n} \nabla \eta_n + O(\mu^2), \tag{23}$$

$$\nabla \cdot \bar{\mathbf{u}}_n = -in\,\eta_n + O(\mu^2). \tag{24}$$

However, before (19) and (20) can be solved, the boundary-layer flow must be analyzed so as to find the expression for the vertical component of the rotational velocity evaluated at the sea bottom; i.e., $u_{\zeta,n}$.

4. Turbulent bottom boundary layer under an oscillatory flow

In the turbulent bottom boundary layer, the eddy viscosity is modeled as a function linearly proportional to the distance from the seafloor, i.e., (1). However, since the frictional velocity, $\boldsymbol{u}_*'$, depends on time, it makes the problem not tractable. Here, we further simplify the eddy viscosity model as

$$\nu'_t(\zeta') = \kappa\langle|\mathbf{u}'_*|\rangle\zeta', \tag{25}$$

in which $\langle\ \rangle$ denotes the average over the fundamental wave period. Introducing a stretched coordinate in the boundary layer

$$\widetilde{\zeta} \equiv \frac{\zeta'}{\widetilde{\delta}'}, \tag{26}$$

where $\widetilde{\delta}'=\langle\delta'(t')\rangle$ is the time averaged boundary-layer thickness, (25) can be expressed as

$$\nu'_t(\zeta') = \widetilde{\zeta}\,\widetilde{\nu}'_0, \tag{27}$$

with

$$\widetilde{\nu}'_0 = \kappa\langle|u'_*|\rangle\,\widetilde{\delta}', \tag{28}$$

being the characteristic eddy viscosity. Since we anticipate that the order of magnitude of the boundary layer thickness is

$$\widetilde{\delta}',= \sqrt{\frac{\widetilde{\nu}'_0}{\omega'_0}}, \tag{29}$$

the scales of eddy viscosity and the boundary layer thickness can be expressed in terms of the averaged bottom stress, $\langle|\tau'_b|\rangle = \rho\langle|\mathbf{u}'_*|\rangle^2$, as

$$\widetilde{\nu}'_0 = \frac{\kappa^2\langle|\tau'_b|\rangle}{\rho'\omega'_0}\text{and}\,\widetilde{\delta}'^2 = \frac{\kappa^2\langle|\tau'_b|\rangle}{\rho'\omega'^2_0}. \tag{30}$$

Therefore, even with the simplifications adopted for the eddy viscosity, the boundary layer thickness as well as the eddy viscosity, can only be determined when the bottom shear stress is solved.

Following LO, the continuity and linearized momentum equations for the rotational velocity components in the boundary layer are, respectively,

$$\nabla\cdot\mathbf{u}_r + \frac{1}{\widetilde{\alpha}u}\frac{\partial u_\zeta}{\partial\widetilde{\zeta}} = 0, \tag{31}$$

and

$$\frac{\partial\mathbf{u}_r}{\partial t} = \frac{\partial}{\partial\widetilde{\zeta}}\left(\widetilde{\zeta}\frac{\partial u_r}{\partial\widetilde{\zeta}}\right) \tag{32}$$

with $\tilde{\alpha}\equiv\widetilde{\delta}'k'_0$. In the present formulation we have adopted the Boussinesq hypothesis $O(\epsilon)\approx O(\mu^2)$ and $O(\tilde{\alpha})\approx O(\mu^4)$ so as to linearize the boundarylayer equations. Hereafter, it is assumed that $O(\tilde{\alpha})\approx O(\epsilon^2)\approx O(\mu^4)$.

Since only periodic motions are considered, we shall also express the rotational velocity inside the boundary layer as a Fourier series in time

$$\mathbf{u}_r\left(\mathbf{x},\widetilde{\zeta},t\right) = \frac{1}{2}\sum_{n=-\infty}^{\infty}\mathbf{u}_{r,n}\left(\mathbf{x},\widetilde{\zeta}\right)\exp(\mathrm{int}), \tag{33}$$

where $\mathbf{u}_{r,-n}$ is the complex conjugate of $\mathbf{u}_{r,n}$. Similarly, the vertical rotational velocity $u\zeta$ and the velocity potential Φ can also be expanded as

$$u_\zeta\left(\mathbf{x},\widetilde{\zeta},t\right) = \frac{1}{2}\sum_{n=-\infty}^{\infty}u_{\zeta,n}\left(\mathbf{x},\widetilde{\zeta}\right)\exp(\mathrm{int}), \tag{34}$$

and

$$\Phi\left(\mathbf{x},\widetilde{\zeta},t\right) = \frac{1}{2}\sum_{n=-\infty}^{\infty}\Phi_n\left(\mathbf{x},\widetilde{\zeta}\right)\exp(\mathrm{int}). \tag{35}$$

The momentum equation for $\mathbf{u}_{r,n}$ is obtained by introducing (33) into (32),

$$in\mathbf{u}_{r,n} = \frac{\partial}{\partial\widetilde{\zeta}}\left(\widetilde{\zeta}\frac{\partial\mathbf{u}_{r,n}}{\partial\widetilde{\zeta}}\right). \tag{36}$$

The no-slip at the bottom requires that,

$$\mathbf{u}_{r,n} = -\nabla\Phi_n \text{ at } \widetilde{\zeta} = \frac{\zeta'_0}{\widetilde{\delta}'}\left[\equiv\widetilde{\zeta}_0\right] \tag{37}$$

with $\zeta'_0\equiv k'_s/30$ and k'_s the equivalent bottom roughness. At the outer edge of the boundary layer, the rotational velocity must vanish, i.e.,

$$\mathbf{u}_{r,n}\rightarrow 0 \text{ at } \widetilde{\zeta}\rightarrow\infty. \tag{38}$$

The solution of the two-point boundary-value problem described by (36)–(38) can be readily obtained (Kajiura, 1964),

$$u_{r,n} = -\nabla\Phi_n\Xi_n^0\left(\widetilde{\zeta}\right) \text{ for } n>0, \tag{39}$$

with

$$\Xi_n^j\left(\widetilde{\zeta}\right)\equiv\frac{K_j\left(2\sqrt{in\,\widetilde{\zeta}}\right)}{K_0\left(2\sqrt{in\,\widetilde{\zeta}_0}\right)}, \tag{40}$$

where K_j is the modified Bessel function of second kind and order j.

Finally, integrating continuity Eq. (31) inside the boundary layer for the n^{th} harmonic, we obtain the leading order vertical rotational velocity at the sea bottom,

$$u_{\zeta,n}\left(\widetilde{\zeta}_0\right) = -\widetilde{\alpha}\mu\nabla^2\Phi_n\frac{1-i}{\sqrt{2n}}\sqrt{\widetilde{\zeta}_0}\,\Xi_n^1\left(\widetilde{\zeta}_0\right) + O\left(\mu^6\right) \tag{41}$$

for $n>0$. We remark that since $\nabla^2\Phi_n=\nabla\cdot\overline{u}_n+O(\mu^2)$, the above equation can be re-written as

$$u_{\zeta,n}\left(\widetilde{\zeta}_0\right) = -\widetilde{\alpha}\mu\nabla\cdot\overline{u}_n\frac{1-i}{\sqrt{2n}}\sqrt{\widetilde{\zeta}_0}\,\Xi_n^1\left(\widetilde{\zeta}_0\right) + O\left(\mu^6\right) \tag{42}$$

for $n>0$. This vertical velocity induced by the boundary layer is used in the depth-integrated continuity equation for irrotational flows in the core region, (20). The effects of the boundary layer are of the order of $O(\mu^3)$. Both $\widetilde{\alpha}(\equiv\widetilde{\delta}'k'_0)$ and $\widetilde{\delta}'$ depend on the bottom stress as shown in (30). In the following section, we present the formulae for bottom stress, τ_b', and the boundary layer thickness, $\widetilde{\delta}'$, so as to close the problem.

4.1. Bottom shear stress and boundary layer thickness

The bottom shear stress in dimensional form is defined as

$$\tau'_b = \rho' v'_t \frac{\partial \mathbf{u}'_r}{\partial \zeta'}\bigg|_{\zeta'=k'_s/30}. \tag{43}$$

The corresponding dimensionless form can be written as

$$\tau_b = \widetilde{\zeta}\frac{\partial \mathbf{u}_r}{\partial \widetilde{\zeta}}\bigg|_{\widetilde{\zeta}=\widetilde{\zeta}_0} \quad \text{with } \tau_b \equiv \frac{\tau'_b}{\widetilde{\alpha}\epsilon\rho' g' h'_0}. \tag{44}$$

Introducing (33) and (39) into (44), the dimensionless bottom stress can be related to the depth-integrated velocity, $\overline{u}_n$, as

$$\tau_b = \sqrt{\frac{k'_s}{30\widetilde{\delta}'}}\sum_{n>0}^{\infty}\Re\left\{\overline{\mathbf{u}}_n\sqrt{in\Xi_n^1\left(\widetilde{\zeta}_0\right)\exp(\mathrm{int})}\right\}, \tag{45}$$

in which $\Re\{\}$ denotes that only the real part is considered. Recalling (30), we obtain a transcendental equation for the boundary layer thickness $\widetilde{\delta}'$ as

$$\widetilde{\delta}'^{3/2} = \frac{\epsilon\kappa^2}{k'_0}\sqrt{\frac{k'_s}{30}}\left\langle\left|\sum_{n>0}^{\infty}\Re\left\{\overline{\mathbf{u}}_n\sqrt{in}\Xi_n^1\left(\widetilde{\zeta}_0\right)\exp(\mathrm{int})\right\}\right|\right\rangle. \tag{46}$$

in which $\widetilde{\zeta}_0$ is a function of $\widetilde{\delta}'$, i.e. (37).

5. Governing equation for the free surface displacement

Once the boundary-layer rotational velocity is related to the depth-integrated velocity in the core region, we can present the Boussinesq-type equations in terms of a single unknown variable, the free surface displacement. Following the procedure presented in Liu et al. (1985), we combine (19) and (20) into a single equation to describe the free surface evolution,

$$\begin{aligned}\varphi_{1,n}\nabla^2\eta_n + \varphi_{2,n}n^2\eta_n \\ = \frac{\epsilon}{2}\sum_{\substack{s\neq n\\ s\neq 0}}\left(n^2-s^2\right)\eta_s\eta_{n-s} - \frac{\epsilon}{2}\sum_{\substack{s\neq n\\ s\neq 0}}\frac{n+s}{n-s}\nabla\eta_s\cdot\nabla\eta_{n-s} \\ -\epsilon\sum_{\substack{s\neq n\\ s\neq 0}}\frac{1}{s(n-s)}\left(\frac{\partial^2\eta_s}{\partial x^2}\frac{\partial^2\eta_{n-s}}{\partial y^2} - \frac{\partial^2\eta_s}{\partial x\partial y}\frac{\partial^2\eta_{n-s}}{\partial x\partial y}\right) + O\left(\mu^4\right),\end{aligned} \tag{47}$$

where

$$\varphi_{1,n}\equiv 1 - \frac{n^2\mu^2}{3}, \tag{48}$$

and

$$\varphi_{2,n}\equiv 1 + \frac{\widetilde{\alpha}}{\mu}\frac{(1-i)}{\sqrt{2n}}\sqrt{\widetilde{\zeta}_0}\Xi_n^1\left(\widetilde{\zeta}_0\right). \tag{49}$$

We note that (23) and (24) have been employed in deriving (47). If the viscous term is neglected (i.e., $\widetilde{\alpha}=0$), (47) reduces to that obtained in Liu et al. (1985). Eq. (47) is a system of nonlinear wave equations for η_n, ($n=1, 2, \ldots$). The nonlinear interactions among different harmonics are included in the right-hand side terms. The boundary layer effects are represented explicitly in the second term of $\varphi_{2,n}$, (49), which will not only reduce the amplitude, but also modify the wave phase. Once η_n is obtained, the depth-integrated velocity $\mathbf{u}_n$, can be found by using (23).

6. Damping and evolution of a modulating periodic wave train in a long channel

Now, we shall examine the damping and evolution of a modulating periodic wave train in a long channel with a constant depth. The free-surface displacement for the n^{th} harmonic, can be written as,

$$\eta_n(x) = A_n(x)\exp(-inx), \tag{50}$$

where A_n (x) is the complex amplitude function. It is well known that because of nonlinear interactions among harmonics the amplitude functions modulate periodically along the channel. Mei and Unluata (1972), have investigated this phenomena without considering the boundary layer effects. Here, we reexamine the problem with the additional consideration of the damping and phase modifications caused by the turbulent boundary layer.

Substituting (50) into (47), we obtain:

$$\begin{aligned}\varphi_{1,n}\left(\frac{d^2A_n}{dx^2} - 2in\frac{dA_n}{dx}\right) + \beta_n n^2 A_n \\ = \frac{\varepsilon n}{2}\sum_{\substack{s\neq n\\ s\neq 0}}(n+s)A_sA_{n-s} \\ -\frac{\varepsilon}{2}\sum_{\substack{s\neq n\\ s\neq 0}}\frac{n+s}{n-s}\left(\frac{dA_s}{dx}\frac{dA_{n-s}}{dx} - isA_s\frac{dA_{n-s}}{dx} - i(n-s)A_{n-s}\frac{dA_s}{dx}\right) \\ +O\left(\mu^4\right),\end{aligned} \tag{51}$$

where

$$\beta_n\equiv\left(\varphi_{2,n}-\varphi_{1,n}\right) = \frac{n^2\mu^2}{3} + \frac{\widetilde{\alpha}}{\mu}\frac{(1-i)}{\sqrt{2n}}\sqrt{\widetilde{\zeta}_0}\Xi_n^1\left(\widetilde{\zeta}_0\right). \tag{52}$$

Moreover, assuming weak amplitude variations in the direction of wave propagation, i.e.,

$$\frac{\partial A_n}{\partial x} = O(\mu^2), \quad \frac{\partial^2 A_n}{\partial x^2} = O(\mu^4), \tag{53}$$

Eq. (51) can be simplified to

$$\frac{dA_n}{dx} = -\frac{in}{2}\beta_n A_n + \frac{i\epsilon}{4}\sum_{\substack{s\neq n\\ s\neq 0}}(n+s)A_s A_{n-s} + O(\mu^4). \tag{54}$$

which is similar to the system of nonlinearly coupled equations obtained by Grataloup and Mei (2003) for the damping of weakly nonlinear waves due to multiple scattering by a randomly rough seabed.

Considering the first 5 harmonics in the wave propagation, the governing equations for the amplitude functions become,

$$\frac{dA_1}{dx} = -\frac{i}{2}\beta_1 A_1 + \frac{3i\epsilon}{4}(A_{-1}A_2 + A_{-2}A_3 + A_{-3}A_4 + A_{-4}A_5), \tag{55}$$

$$\frac{dA_2}{dx} = -\frac{2i}{2}\beta_2 A_2 + \frac{6i\epsilon}{4}\left(\frac{1}{2}A_1^2 + A_{-1}A_3 + A_{-2}A_4 + A_{-3}A_5\right), \tag{56}$$

$$\frac{dA_3}{dx} = -\frac{3i}{2}\beta_3 A_3 + \frac{9i\epsilon}{4}(A_1A_2 + A_{-1}A_4 + A_{-2}A_5), \tag{57}$$

$$\frac{dA_4}{dx} = -\frac{4i}{2}\beta_4 A_4 + \frac{12i\epsilon}{4}\left(\frac{1}{2}A_2^2 + A_1A_3 + A_{-1}A_5\right), \tag{58}$$

$$\frac{dA_5}{dx} = -\frac{5i}{2}\beta_5 A_5 + \frac{15i\epsilon}{4}(A_2A_3 + A_1A_4), \tag{59}$$

which are accurate up to O(μ^4).

6.1. Boundary layer thickness and an iterative procedure

The bottom boundary layer effect term, $\varphi_{2,n}$, in (55)–(59) is a function of the non-dimensional parameters $\widetilde{\zeta}_0 = k_s'/30\,\widetilde{\delta}'$ and $\widetilde{\alpha} \equiv \widetilde{\delta}' k_0'$, which are part of solutions. An iterative procedure is adopted to find the solutions. Initial guesses (constant values) for $\widetilde{\zeta}_0$ and $\widetilde{\alpha}$ are made so as to calculate $\Xi_n^1(\widetilde{\zeta}_0)$ in (49). The system of nonlinear ordinary differential Eqs. (55)–(59), is then solved numerically with an implicit finite difference scheme. Once the free surface elevation for the n^{th} harmonic, η_n, is obtained, using the relation (23) the leading order of the depth averaged velocity $\overline{\mathbf{u}}_n$ can be computed. The non-dimensional parameter $\widetilde{\zeta}_0$ is then updated by applying (46), which can also be expressed as Eq. (60).

$$\widetilde{\zeta}_0 = \left\{\frac{30\epsilon\kappa^2}{\varrho}\left\langle\left|\sum_{n>0}^{\infty}\Re\left\{\overline{\mathbf{u}}_n\sqrt{in}\,\Xi_n^1\left(\widetilde{\zeta}_0\right)\exp(\mathrm{int})\right\}\right|\right\rangle\right\}^{-2/3}. \tag{60}$$

with $\varrho \equiv k_0' k_s'$. The new value $\widetilde{\zeta}_0$ is used to update $\widetilde{\alpha}$, for $\widetilde{\alpha} = \varrho/30\,\widetilde{\zeta}_0$. The procedure described above is repeated until a converge criteria between two successive iterations is reached (the relative error between two successive iterations is smaller than 10^{-3} for all x).

6.2. Results

In the numerical example, a wave maker, located at $x=0$, generates a sinusoidal wave train with $A_1(0)=1$ and $A_2(0)=A_3(0)=A_4(0)=A_5(0)=0$. The values for the nonlinear parameter and the frequency dispersion are $\varepsilon=0.1$, and $\mu^2=0.1216$, respectively. The bottom roughness is specified by $\varrho \equiv k_0' k_s' = 10^{-4}$. The initial guesses are made for $\widetilde{\zeta}_0=0.01$ and $\widetilde{\alpha}=3.3\cdot10^{-4}$ for all x positions.

The amplitude variation for the first five harmonics is shown in Fig. 1. The grey lines correspond to the classical solution where the viscous terms are neglected (i.e., $\widetilde{\alpha}=0$). The solutions considering the boundary layer effects are displayed as black lines. In both situations, as the wave train propagates into the channel, wave energy is transferred from the first to higher harmonics as the result of the nonlinearity in (55)–(59). However, when the turbulent boundary layer effects are included, the viscous damping reduces the amplitudes for all harmonics. The boundary layer also affects the phases of each harmonic resulting in different phase speed. It is quite obvious that the boundary layer effects are accumulative. Those effects could become very significant if the wave train propagates a long distance. In Fig. 2, a snapshot of the depthaveraged velocity $\overline{u}$ and dimensionless boundary layer thickness, $\widetilde{\zeta}_0$, along the channel at $t=0$.

To further illustrate the boundary layer effects, the time histories of the freesurface elevation at the nondimensional locations $x=20$ and $x=120$ are shown in Fig. 3. The grey lines correspond to the inviscid solutions where $\widetilde{\alpha}=0$ and the black lines denote the solutions with the effects of the boundary layer included. Since the boundary-layer dissipative effect is accumulative, near the wavemaker (top panel in Fig. 3), the wave train has not been significantly influenced by the boundary layer and both solutions are almost identical. However, as the wave train propagates farther down the channel (bottom panel in Fig. 3), the dissipative effects reduce the wave amplitude. The phase shifts in the wave form are also obvious.

To compare the present results with the traditional formulation in which a bottom stress term is added in the momentum equations, a companion model has also been developed (see Appendix). In the traditional model, the bottom stress is assumed to be in phase with the bottom velocity and a frictional coefficient is estimated from the empirical formula suggested by Nielsen (1992). This frictional coefficient is a function of the bottom roughness and the near bottom orbital displacement (a_b'). The time history of the depth-averaged velocity $\overline{u}$ at $x=120$ obtained from (54) where $\varphi_{2,n}$ is given by (49) is presented in Fig. 4 (top panel) in black together with the velocity obtained from the traditional approach (61), in grey. The bottom shear stress τ_b from (45) is displayed in black in the bottom panel of Fig. 4 together with the bottom stress from

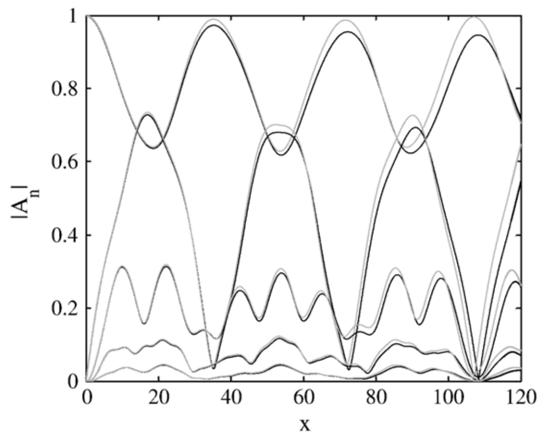

Fig. 1. Amplitudes of the modulated wave train with five harmonics. The grey lines correspond to the results without the viscous effects and black lines are results with the boundary layer effects included.

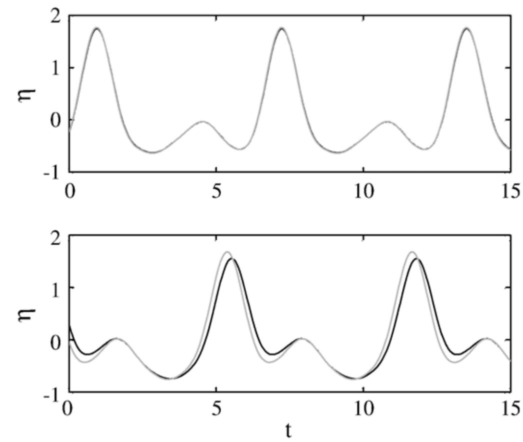

Fig. 3. Time histories of the free surface elevations at $x=0$ (top panel), and at $x=120$ (bottom panel) for a wave train propagating without damping (grey) and with the turbulent boundary layer effects (black).

traditional approach (66), in grey where $\varphi_{2,n}$ is given by (64). Using the traditional formulation with the proper selection of frictional coefficient, the effects of boundary layer on wave propagation are quite similar to those obtained from the present formulation for the present case. However, these two models predict very different bottom stress as shown in Fig. 4 (grey lines). The bottom stress, in turn, will have significant impacts on estimating sediment transport.

7. Concluding remarks

In the present paper a new Boussinesq-type model for periodic wave propagation has been developed when the effects of a turbulent boundary layer are significant. In this model the eddy viscosity model is used in the turbulent boundary layer and is further approximated as a linear function of the distance measured from the seafloor. The analytical expressions for the boundary-layer velocity can be found in terms of the irrotational velocity in the core region and the effects of the boundary layer appear in the depth-integrated continuity equation. The bottom stress, the boundary layer thickness and the magnitude of the turbulent eddy viscosity are part of solutions. An iterative scheme is introduced to solve the system of equations. Numerical solutions for the evolution of periodic waves propagating in a one-dimensional channel are discussed. The

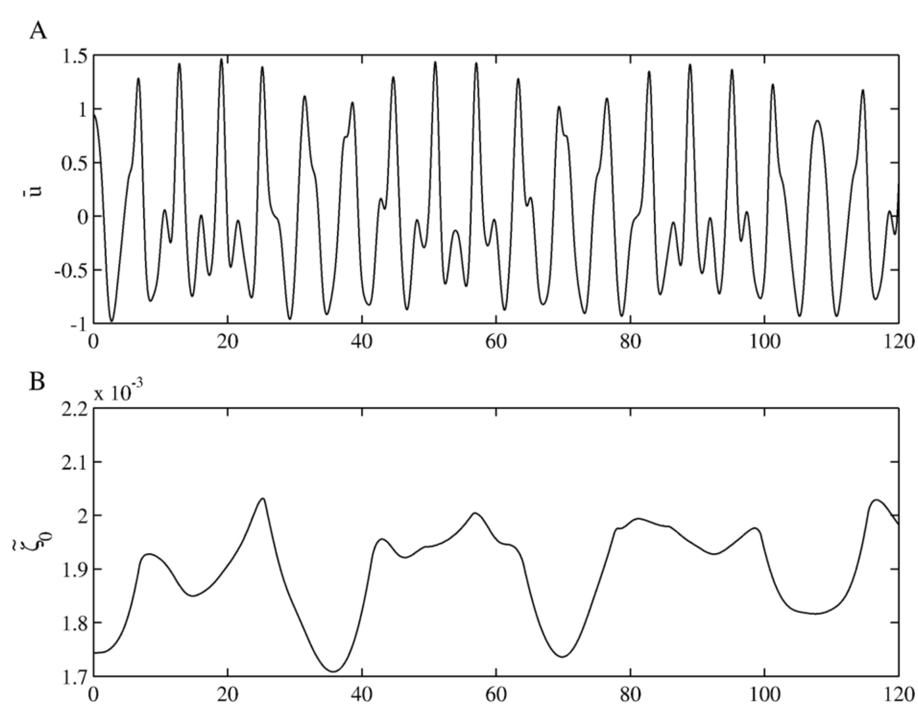

Fig. 2. A) The depth-averaged velocity $\bar{u}$ along the wave channel at $t=0$. B) Distribution of $\tilde{\zeta}_0$. The characteristics of the wave motion are defined by, $\mu^2=0.1216$, $\varepsilon=0.1$ and $\varrho=10^{-4}$.

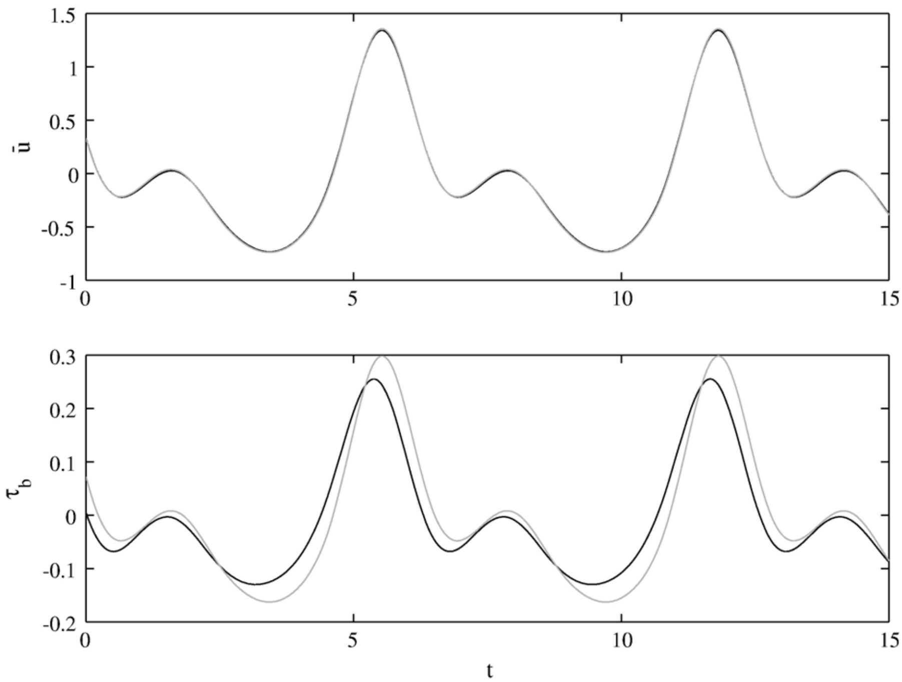

Fig. 4. Time histories of depth integrated velocity in dimensionless form at $x=120$ (top panel) from the present approach (black) using (49) and from the traditional approach (64) (grey). The time history of bottom stress from (45) is presented in grey (bottom panel) together with the bottom stress calculated from (66). The frictional coefficient for the traditional approach sused $C_f=0.0037$.

model can be extended and implemented straightforwardly for two-dimensional problems.

Acknowledgments

AO would like to thank financial support from MEC trough the postdoctoral grant at Cornell University (EX2003-0430) and Govern Balear, UGI6ZC project. GS was supported by the visiting professor program from UCLM. PLFL would like to acknowledge the support from National Science Foundation through various grants to Cornell University.

Appendix

The viscous effects induced by the bottom boundary layer have been traditionally included in the momentum equation as

$$\frac{\partial \bar{\mathbf{u}}'}{\partial t'} + \frac{1}{2}\nabla'(\bar{\mathbf{u}}' \cdot \bar{\mathbf{u}}') + g'\nabla'\eta' - \frac{h'^2}{3}\nabla'\left(\nabla' \cdot \frac{\partial \bar{\mathbf{u}}'}{\partial t'}\right) = -\frac{\boldsymbol{\tau}'_b}{\rho' h'} \tag{61}$$

where $\boldsymbol{\tau}'_b$ is the bottom shear stress for which we parameterize as,

$$\boldsymbol{\tau}'_b = C_f \rho' u'_c \mathbf{u}' \tag{62}$$

where C_f is the frictional coefficient, u'_c a characteristic velocity and $\mathbf{u}'$ the near bottom orbital velocity. We remark here that the use of a characteristic velocity is employed, instead of $|\mathbf{u}'|$, is for the convenience of obtaining the solution in the frequency domain. The continuity equation in dimensional form reads,

$$\nabla' \cdot \{(h' + \eta')\bar{u}'\} + \frac{\partial \eta'}{\partial t'} = 0 \tag{63}$$

Assuming periodic motions in time and following the same approach as the one employed in this paper, we obtain the same expression for the free surface elevation as (47) but with the viscous term $\varphi_{2,n}$ being expressed as,

$$\varphi_{2,n} = 1 - \frac{i\epsilon C_f}{n\mu} \tag{64}$$

We note that $u'_c = \epsilon\sqrt{g'h'}$ has been used. The friction coefficient C_f is obtained using the empirical formula (Nielsen, 1992):

$$C_f = \frac{1}{2}\exp\left(5.5\left(\frac{k'_s}{a'_b}\right)^{0.2} - 6.3\right) \approx \frac{1}{2}\exp\left(5.5\left(\frac{\varrho}{\epsilon}\right)^{0.2} - 6.3\right) \tag{65}$$

For the example presented in this paper $C_f = 0.0037$. To compare the bottom stress obtained from two models, the dimensional bottom stress, (62), is normalized by the same parameters used in the present formulation,

$$\boldsymbol{\tau}_b = \frac{30 C_f \epsilon \tilde{\zeta}_0}{\varrho}\mathbf{u} \tag{66}$$

References

Grant, W.D., Madsen, O.S., 1979. Combined wave and current interaction with a rough bottom. Journal Geophysical Research 84, 1797–1808.

Grataloup, G.L., Mei, C.C., 2003. Localization of harmonics generated in nonlinear shallow water waves. Physical Review E 68, 026314.

Jonsson, I.G., Carlsen, N.A., 1976. Experimental and theoretical investigations in an oscillatory rough turbulent boundary. Journal Hydraulic Research 14, 45–60.

Kajiura, K.A., 1968. A model of the bottom boundary layer in water waves. Bulletin of the Earthquake Research Institute, University of Tokyo 46, 75–123.

Lighthill, M.J., 1978. Waves in Fluids. Cambridge University Press.

Liu, P.L.-F., 2006. Turbulent boundary layer effects on transient wave propagation in shallow water. Proceeding of the Royal Society of London 462 (2075), 3481–3491.

Liu, P.L.-F., Orfila, A., 2004. Viscous effects on transient long-wave propagation. Journal Fluid Mechanics, 520, 83–92.

Liu, P.L.-F., Yoon, S.B., Kirby, J.T., 1985. Nonlinear refraction diffraction of waves in shallow water. Journal Fluid Mechanics 153, 185–201.

Liu, P.L.-F., Simarro, G., Vandever, J., Orfila, A., 2006. Experimental and numerical investigation of viscous effects on solitary wave propagation in a wave tank. Coastal Engineering 53 (2-3), 81–190.

Liu, P.L.-F., Park, Y.S., Cowen, E.A., 2007. Boundary layer flow and bed shear stress under a solitary wave. Journal of Fluid Mechanics 574, 449–463.

Mei, C.C., Unluata, U., 1972. Harmonic Generation in Shallow Water Waves. In: Meyer, R.E. (Ed.), Waves on Beaches and Resulting Sediment Transport. Academic Press, New York, pp. 181–202.

Mei, C.C., 1989. The applied dynamic of ocean surface waves. World Scientific, Singapore. 324 pp.

Nielsen, P., 1992. Coastal Boundary Layers and Sediment Transport. World Scientific, Singapore. 324 pp.

Torsvik, T., Liu, P.L.-F., 2007. An efficient method for the numerical calculation of viscous effects on transient long-waves. Coastal Engineering 54, 263–269.